Seismic dip estimation based on the two-dimensional Hilbert transform and its application in random noise attenuation[a]

[a]Published in Applied Geophysics, 12, 55-63 (March 2015)

*Cai Liu**, *Changle Chen**, *Dian Wang*‡*, *Yang Liu**, *Shiyu Wang**, *and Liang Zhang*†

ABSTRACT

In seismic data processing, random noise seriously affects the seismic data quality and subsequently the interpretation. This study aims to increase the signal-to-noise ratio by suppressing random noise and improve the accuracy of seismic data interpretation without losing useful information. Hence, we propose a structure-oriented polynomial fitting filter. At the core of structure-oriented filtering is the characterization of the structural trend and the realization of nonstationary filtering. First, we analyze the relation of the frequency response between two-dimensional (2D) derivatives and the 2D Hilbert transform (Riesz transform). Then, we derive the noniterative seismic local dip operator using the 2D Hilbert transform to obtain the structural trend. Second, we select polynomial fitting as the nonstationary filtering method and expand the application range of the nonstationary polynomial fitting. Finally, we apply variableamplitude polynomial fitting along the direction of the dip to improve the adaptive structureoriented filtering. Model and field seismic data show that the proposed method suppresses the seismic noise while protecting structural information.

INTRODUCTION

Random noise, which refers to any unwanted features in data, commonly contaminates seismic data. Random noise sources in seismic exploration are roughly divided into three categories. First, there are external disturbances such as wind and human activities. Second, there is electronic instrument noise. Third, there is the irregular interference owing to seismic explosions. Random noise attenuation is a significant step in seismic data processing. In particular, the extent of noise suppression in poststack data directly affects the accuracy of subsequent processing and interpretation. Presently, several different random noise attenuation methods are available. Liu

**College of Geo-exploration Science and Technology, Jilin University, Changchun 130026, China.*
†*Qian An Oil Factory, Jilin Oilfield, CNPC, Songyuan 138000, China.*
‡*Corresponding Author: Dian Wang (Email: dianwang@jlu.edu.cn)*

et al. (2006) presented a 2D multilevel median filter for random noise attenuation, whereas Liu et al. (2009b) used a 1D time-varying window median filter. Bekara and van der Baan (2009) used the empirical mode decomposition (EMD) method and proposed a filtering technique for random noise attenuation in seismic data. Liu et al. (2009a) proposed a high-order seislet transform for random noise attenuation. Li et al. (2012) applied morphological component analysis to suppress random noise and Liu et al. (2012) proposed a novel method of random noise attenuation based on local frequency-domain singular value decomposition (SVD). Maraschini and Turton (2013) assessed the effect of nonlocal means random noise attenuator on coherency. Li et al. (2013) used time-frequency peak filtering to suppress strong noise in seismic data. Liu and Chen (2013) used f-x regularized nonstationary autoregression to suppress random noise in 3D seismic data. The abovementioned random noise attenuation methods are limited by their lack of protection of structural information. For example, improper filtering may blur small faults, which may also make the displacement of larger fault continuous and consequently make layers appear continuous instead of faulted. Obviously, this hinders fault interpretation, and makes denoising and protecting structural information important. Fehmers and Hocker (2003) applied structureoriented filtering to fast structural interpretation. Hoeber et al. (2006) applied nonlinear filters, such as median, trimmed mean, and adaptive Gaussian, over planar surfaces parallel to the structural dip. Fomel and Guitton (2006) suggested the method of plane-wave construction by using model reparameterization. Liu et al. (2010) applied nonlinear structure-enhancing filtering by using plane-wave prediction to preserve structural information. Liu et al. (2011b) proposed a poststack random noise attenuation method by using weighted median filter based on local correlation and tried to balance the protection of fault information and noise attenuation.

Structure-oriented filtering includes structure prediction and filtering. Seismic dip is at the core of structure prediction; for, we can use seismic dip to determine structural trends and achieve structure protection. Ottolini (1983) used local slant stack to formulate a local seismic dip estimation method. Fomel (2002) proposed a seismic dip estimation method based on the plane-wave destruction (PWD) filter. Schleicher et al. (2009) compared different methods of local dip computations. The selection of filtering methods in structure-oriented filters is critical and polynomial fitting has been successfully applied to seismic data denoising. Lu and Lu (2009) used edge-preserving polynomial fitting to suppress random seismic noise. This method achieves better results when the trajectories of seismic events are linear or the amplitudes along the trajectories are not constant. Liu et al. (2011a) proposed a novel seismic noise attenuation method by using nonstationary polynomial fitting (Fomel, 2009) and shaping regularization (Fomel, 2007) for constraining the smoothness of the polynomial coefficients.

In this paper, we discuss the two-dimensional (2D) Hilbert transform and use it to derive the formula for the dip in the plane wave, construct a stable algorithm for estimating the dip, and improve the computational efficiency of Fomel's method (Fomel, 2002) without minimizing the precision of the dip estimation. Finally, we use synthetic model and field seismic data to demonstrate the applicability of the proposed method.

THEORY

The extraction of structural information and the selection of effective filtering methods are critical to structure-oriented filters. Because of the time-space relation in seismic data, structural information must satisfy kinematics and kinetics equations. The dip of seismic events reveals structural features. This study is the first to discuss a calculation method for the local seismic dip.

Noniterative local dip calculation

Following the local plane-wave equation (Fomel, 2002)

$$\frac{\partial P(x,t)}{\partial x} + \sigma(x,t)\frac{\partial P(x,t)}{\partial t} = 0, \tag{1}$$

we define the local dip of seismic data

$$\sigma(x,t) = -\frac{\partial P(x,t)}{\partial x} / \frac{\partial P(x,t)}{\partial t}, \tag{2}$$

where $P(x,t)$ is the seismic wave field and $\sigma(x,t)$ is the local seismic dip as a function of time t and distance x. However, in actual computations, because the local dip is used to determine the direction of a seismic event, we ignore the dimensions and sampling interval; thus, σ only depends on the sampling data and the local dimensionless dip is defined as

$$\sigma = -(\frac{\partial P(x,t)}{\partial x} / \frac{\partial P(x,t)}{\partial t}) \cdot \frac{\Delta x}{\Delta t} = -\frac{\partial P}{\partial x} / \frac{\partial P}{\partial y}, \tag{3}$$

where $\partial P/\partial x$ and $\partial P/\partial y$ are the partial derivatives of the seismic wave field in the $x-$ and $y-$direction, respectively, and Δx and Δt are the respective sampling intervals in the $x-$ and $y-$direction.

Using equation 3, we compute the local dip by using the specific values of the space- and time-directional derivatives. Hence, we first discuss the derivative operator.

The ideal differentiator frequency response is

$$F_{IDD}(\omega) = i\omega, -\pi \leq \omega \leq \pi. \tag{4}$$

The ideal differentiator frequency response is multiplied by a frequency-dependent linear function in the frequency domain. The direct calculation of the derivative of the signal in the time domain enhances the high-frequency random noise and reduces the dip accuracy. Thus, we analyze the frequency response of the derivative operator and the frequency response of the Hilbert transform. We derive the Hilbert transform (Appendix A) and the approximate partial derivative by using the finite impulse response (FIR) filter (Pei and Wang, 2001). We use a 2D Hilbert transform to approximate the partial derivatives of the wave field, which reduces the side effect of strong high-frequency random noise owing to the derivative algorithm.

The redefined noniterative local dip of the seismic data is

$$\sigma = -(\frac{\partial P}{\partial x}/\frac{\partial P}{\partial y}) = -\frac{FFT^{-1}[\tilde{P}(x)]}{FFT^{-1}[\tilde{P}(y)]} = -\frac{FFT^{-1}[\frac{1}{\sqrt{c_x}}\tilde{P}(x)]}{FFT^{-1}[\frac{1}{\sqrt{c_y}}\tilde{P}(y)]} \approx -\frac{FFT^{-1}[H_{HT}(x)]}{FFT^{-1}[H_{HT}(y)]} \approx -\frac{H_{HTx}}{H_{HTy}}, \tag{5}$$

where $\tilde{P}(x)$ is the frequency response function of the partial derivative in the $x-$direction and $\tilde{P}(y)$ is the frequency response function of the partial derivative in the $y-$direction. The dimensions are ignored in the derivation and c does not depend on the time and space sampling intervals; thus, we take $c_x = c_y$. $H_{HT}(x)$ is the frequency response function of the Hilbert transform in the $x-$direction and $H_{HT}(y)$ is the frequency response function of the Hilbert transform in the $y-$direction. H_{HTx} and H_{HTy} are the components of the 2D Hilbert transform in the $x-$ and $y-$direction, respectively. Using equation 5, we calculate the local seismic dip attribute by using the 2D Hilbert transform instead of the derivative operation. Because division is required in equation 5 and the denominator might become zero, we add the nonzero constant ε in the denominator

$$\sigma \approx -\frac{H_{HTx}}{H_{HTy} + \varepsilon}. \tag{6}$$

Fomel (2007) proposed the shaping regularization for imposing regularization constraints in estimation problems and defined the local seismic attributes. In this paper, we use the same method to constrain the division and smooth the local dip by using the Gaussian smooth operator as the regularization operator.

To show the validity of the proposed dip calculation method, we construct a synthetic seismic model and add white Gaussian random noise, as shown in Figure 1a. The components of the 2D Hilbert transform in the $x-$ and $y-$direction are shown in Figures 1b and 1c, respectively. We obtain the dip of the seismic data by using the ratio of the two components and calculate the smoothing constraints, as shown in Figure 1d. We see that the calculation results can accurately reflect the dip value of the original data at different locations, such as the tilted layers at the top the underlying strata with the sinusoidal fluctuations, and the fault location. Using the 2D Hilbert transform and shaping regularization, we obtain the smooth local dip attribute.

Another effective calculation method of the time-varying and space-variant seismic local dip is based on the plan-wave destruction (PWD) filter proposed by Fomel (2002). The PWD filter realizes the plane-wave propagation across different traces, while the total energy of the propagating wave stays invariant, by using an all-pass digital filter in the time domain and a Taylor expansion of the all-pass filter frequency.

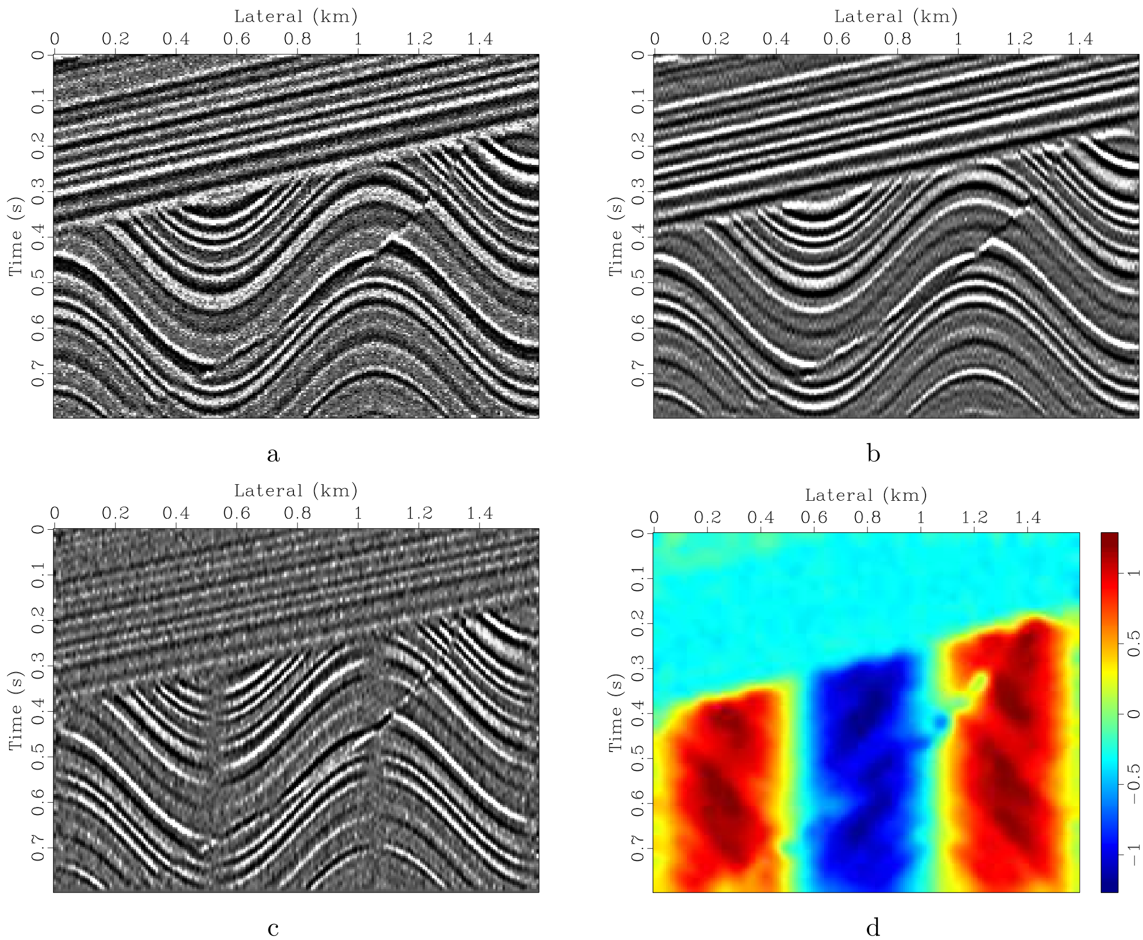

Figure 1: Local seismic dip based on the 2D Hilbert transform. Synthetic seismic data (a), time component of the 2D Hilbert transform (b), space component of the 2D Hilbert transform (c), and local seismic dip (d).

We obtain the relation of the PWD and space-time-varying local seismic dip by using the Gauss-Newton algorithm to solve the nonlinear problem of local seismic dip. This method can be essentially understood as solving an implicit finite-difference scheme for the local planewave equation. The disadvantage of the PWD-based calculation method is its slow computation speed, which is especially worse at higher order conditions. The computational cost of the proposed method is proportional to $2N_x \times N_t$, where $N_x \times N_t$ is the data size, whereas the computational efficiency of the PWD-based dip estimation method is proportional to $N_{iter} \times N_x \times N_t$, where N_{iter} is the number of iterations. Hence, to achieve similar accuracy, the dip estimation method based on the 2D Hilbert transform requires a smaller number of iterations than the PWD-based method.

The dip of seismic events controls the trend of the constructed seismic model; thus, next, we need to apply filtering along the trend. The selected filtering method must simultaneously suppress the seismic noise and protect structural information.

Nonstationary polynomial fitting

Traditional stationary regression is used to estimate the coefficients $a_i, i = 1, 2, \ldots, N$ by minimizing the prediction error between a "master" signal s($\mathbf{x}$) (where $\mathbf{x}$ represents the coordinates of a multidimensional space) and a collection of slave signals $L_i(\mathbf{x}), i = 1, 2, \ldots, N$ (Fomel, 2009)

$$E(\mathbf{x}) = s(\mathbf{x}) - \sum_{i=1}^{N} a_i L_i(\mathbf{x}). \tag{7}$$

When $\mathbf{x}$ is 1D and $N = 2$, $L_1(\mathbf{x}) = 1$ and $L_2(\mathbf{x}) = x$, the problem of minimizing $E(\mathbf{x})$ amounts to fitting a straight line $a_1 + a_1 x$ to the master signal. Nonstationary regression is similar to equation 7 but allows the coefficients $a_i(\mathbf{x})$ to vary with $\mathbf{x}$, and the error (Fomel, 2009)

$$E(\mathbf{x}) = s(\mathbf{x}) - \sum_{i=1}^{N} a_i(\mathbf{x}) L_i(\mathbf{x}) \tag{8}$$

is minimized to solve for the multinomial coefficients $a_i(\mathbf{x})$. The minimization becomes an ill-posed problem because $a_i(\mathbf{x})$ rely on the independent variables $\mathbf{x}$. To solve the ill-posed problem, we constrain the coefficients $a_i(\mathbf{x})$. Tikhonov's regularization (Tikhonov, 1963) is a classical regularization method that amounts to the minimization of the following functional (Fomel, 2009)

$$F(a) = \|E(\mathbf{x})\|^2 + \varepsilon^2 \sum_{i=1}^{N} \|\mathbf{D}[a_i(\mathbf{x})]\|^2, \tag{9}$$

where $\mathbf{D}$ is the regularization operator and ε is a scalar regularization parameter. When $\mathbf{D}$ is a linear operator, the least-squares estimation reduces to linear inversion

(Fomel, 2009)

$$\mathbf{a} = \mathbf{A}^{-1}\mathbf{d}, \tag{10}$$

where

$$\mathbf{a} = [a_1(x)a_2(x)\cdots a_N(x)]^T,$$
$$\mathbf{d} = [L_1(x)s(x)L_2(x)s(x)\cdots L_N(x)s(x)]^T,$$

and the elements of matrix $\mathbf{A}$ are

$$A_{ij}(\mathbf{x}) = L_i(\mathbf{x})L_j(\mathbf{x}) + \varepsilon^2\delta_{ij}\mathbf{D}^T\mathbf{D}\ .$$

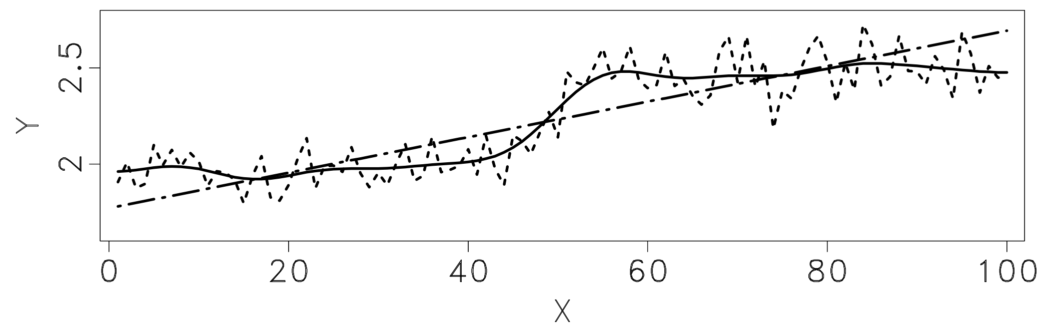

Figure 2: Least-squares linear fitting compared with nonstationary polynomial fitting.

Next, we use a simple signal to simulate the variation of the amplitude of a nonstationary event with random noise (dashed line in Figure 2). In Figure 2, the dot dashed line denotes the results of the least-squares linear fitting and the solid line denotes the results of the nonstationary polynomial fitting. We compare the least-squares linear fitting and nonstationary polynomial fitting results, and we find that the nonstationary polynomial fitting models the curve variations more accurately for events with variable amplitude, particularly for $40 < x < 60$.

SYNTHETIC DATA TESTS

We construct a new structure-oriented filtering method based on the 2D Hilbert transform with nonstationary polynomial fitting and apply it to synthetic data (Figure 1a). The local seismic dip (Figure 1d) controls the trend of the event, and we apply nonstationary polynomial fitting along the direction of the dip for fast structural interpretation using structure-oriented filtering. We achieve continuous model protection in the direction of dip, and noise attenuation and fault protection because of the use of nonstationary polynomial fitting. Nine sampling points are used in the structure-oriented filtering and five sampling points in the nonstationary polynomial fitting. The filtering results are shown in Figure 3a and the difference profile is shown in Figure 3b. Figure 3a shows that the upper tilted layer, the lower sinusoidal layer, and the fault information are preserved, while the noise is clearly suppressed. Random noise constitutes most of the difference profile without any tilted layer and fault

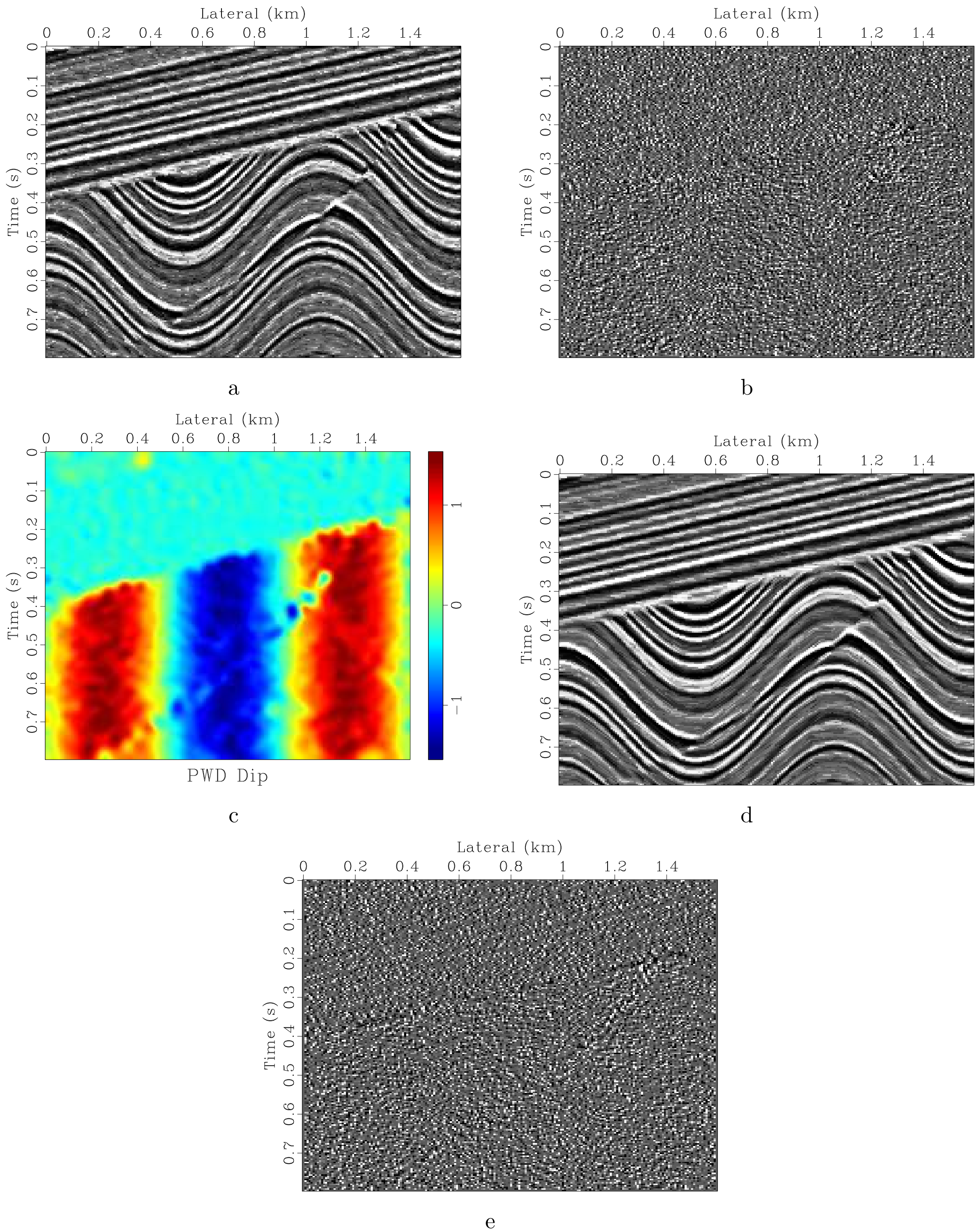

Figure 3: Analysis of results using different structure-oriented filtering. Nonstationary polynomial fitting (a), difference profile of nonstationary polynomial fitting (b), local PWD-based dip (c), median filter (d), and difference profile of median filter (e).

information left because the local seismic dip cannot reflect the trend of the layers and owing to the attenuation of the limited effective information. To compare the proposed method with the PWD-based local dip estimation method (Figure 3c) with similar dip accuracy (Figure 1d), we choose the median filter and show the results in Figure 3d and the difference profile in Figure 3e. We compare the two profiles after the application of the median filter. We find more useful structural information than the method we proposed. That means the method we proposed has better effect.

FIELD DATA TESTS

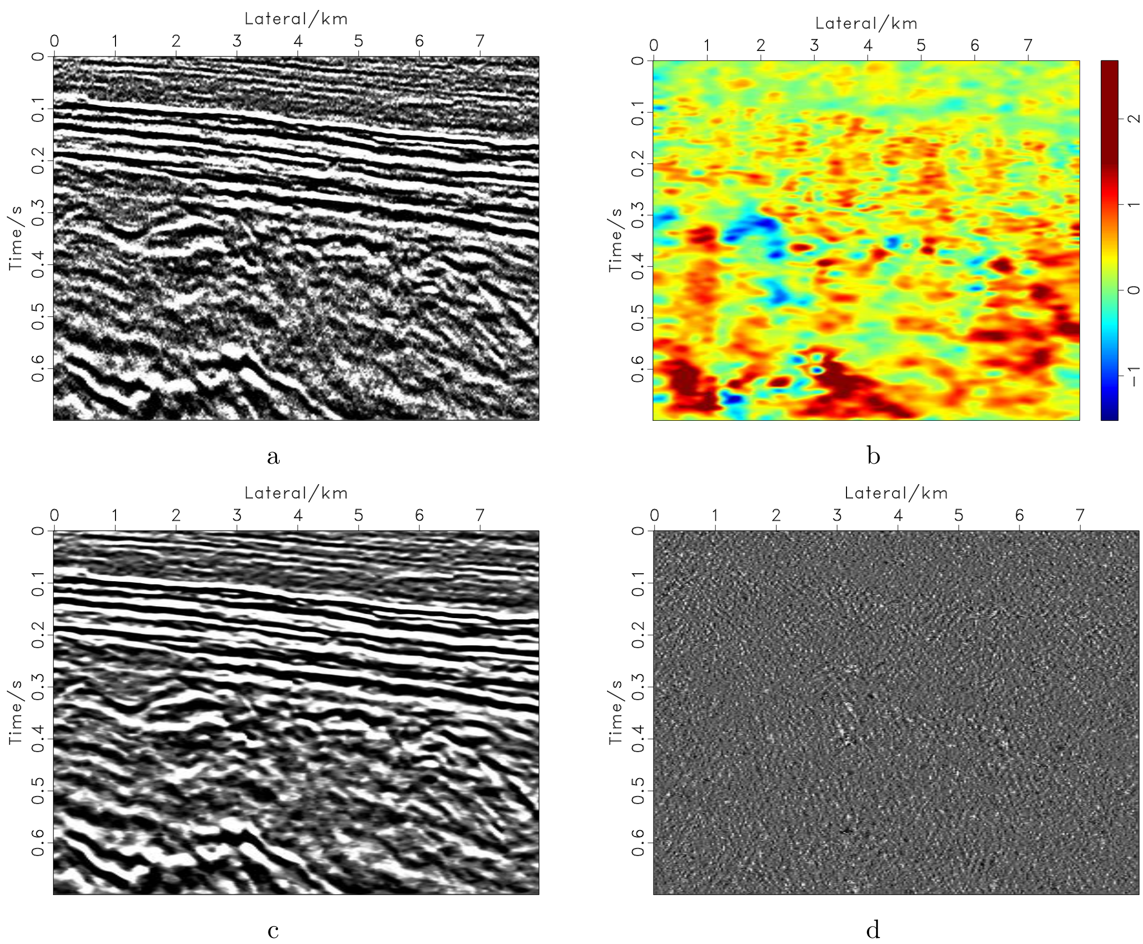

Figure 4: Comparison of processing results. Field data (a), Local dip (b), After filtering (c), Difference profile (d).

For field data processing, we chose the 2D profile of 3D poststack data (Liu and Chen, 2013). The shallow structures are simple planar layers and the deep structures are complex curved layers. First, we use the proposed method, which is based on the 2D Hilbert transform, to compute the corresponding local seismic dip attribute (Figure 4b). From Figure 4b, we see that the dip changes smoothly and steadily in the midshallow layer corresponding to the continuous event in the profile, whereas the variation of the dip in the deep layer is relatively larger, which characterizes the bending event in the mid-deep layer.

The trend of the local seismic events can be determined by using the dip attribute; thus, we select the filtering window, which is determined by the dip, and use nonstationary polynomial fitting for filter processing. The window size of the structure-oriented data consists of 11 sampling points and the window size of the nonstationary polynomial fitting comprises seven sampling points.

Figure 4c shows the denoising results. We see that the random noise in the raw profile is suppressed, the whole section is clearer, and the continuity of the plane event (0.1s-0.3s) in the shallow layer and the curved event (below 0.3s) in the deep layer has improved. The difference profile (Figure 4d) shows that the removed noise is mainly irrelevant random noise and the information is well preserved.

CONCLUSIONS

We propose a seismic dip estimate method based on the 2D Hilbert transform. We compute the stable dip by using the noniterative approximation relation within the middle frequency band, and improve the computational efficiency relative to the iterative dip algorithm based on the PWD filter. We combine the proposed method with nonstationary polynomial fitting to suppress the seismic random noise using the computed local seismic dip. We predict the seismic structure trend using the structure-oriented window based on the seismic dip, while balancing the random noise attenuation and signal preservation via filtering with the nonstationary polynomial fitting. The proposed method suppresses the seismic noise and strongly depend on the of dip trend prediction. The accuracy of computed dip is directly affected by filtering. The method is not applicable at strong noise conditions. We use synthetic model and field data processing, to demonstrate the applicability of the proposed method.

APPENDIX A: HILBERT TRANSFORM DERIVATION FOR APPROXIMATING THE PARTIAL DERIVATIVE

Derivation of the FIR transfer function for the frequency response of digital differentiators

First, to characterize the FIR for signal differentiators, we transform the Leibniz series $\frac{2\text{arcsin}x}{\sqrt{1-x^2}}$ to power series (Lehmer, 1985)

$$\frac{2\text{arcsin}x}{\sqrt{1-x^2}} = 2x\left[1+\sum_{m=1}^{\infty}\frac{(2\text{m})!!}{(2\text{m}+1)!!}x^{2m}\right]. \tag{A-1}$$

We substitute $\sin(\frac{\omega}{2})$ for x, and after rearrangement and truncation of the first M terms, we obtain

$$\begin{aligned}
&\frac{\omega}{\sqrt{1-\sin^2\frac{\omega}{2}}} \\
&= 2\sin\frac{\omega}{2}\left[1+\sum_{m=1}^{M}\frac{(2\mathrm{m})!!}{(2\mathrm{m}+1)!!}\left(\frac{1-\cos\omega}{2}\right)^m + o((\frac{1-\cos\omega}{2})^{M+1})\right]
\end{aligned} \tag{A-2}$$

and after manipulation

$$\begin{aligned}
\omega &= 2\sin\frac{\omega}{2}\cos\frac{\omega}{2}\left[1+\sum_{m=1}^{M}\frac{(2\mathrm{m})!!}{(2\mathrm{m}+1)!!}\left(\frac{1-\cos\omega}{2}\right)^m + o((\frac{1-\cos\omega}{2})^{M+1})\right] \\
&= \sin\omega\left[1+\sum_{m=1}^{M}\frac{(2\mathrm{m})!!}{(2\mathrm{m}+1)!!}\left(\frac{1-\cos\omega}{2}\right)^m + o((\frac{1-\cos\omega}{2})^{M+1})\right].
\end{aligned} \tag{A-3}$$

We ignore the higher order terms and we obtain the $(2M+2)$th-order causal transfer function of the derivative operator as

$$\hat{F}_{DD}(z) \approx -\frac{1-z^{-2}}{2}\left\{z^{-M}+\sum_{m=1}^{M}\frac{(2\mathrm{m})!!}{(2\mathrm{m}+1)!!}\cdot z^{-(M-m)}\left[-\frac{(1-z^{-1})^2}{4}\right]^m\right\}. \tag{A-4}$$

Derivation of the FIR transfer function for the frequency response of the Hilbert transform

The ideal frequency response of the Hilbert transform is expressed as

$$H_{IHT}(\omega) = -i\,\mathrm{sgn}\,\omega = -i\frac{\omega}{|\omega|} = \begin{cases} i, & -\pi<\omega<0 \\ -i, & 0<\omega<\pi \end{cases}. \tag{A-5}$$

From equations 4 and A-5, we obtain the difference as $1/|\omega|$. For

$$\mathrm{sgn}\,x = \frac{x}{\sqrt{x^2}} = xf(x^2), x\neq 0 \tag{A-6}$$

and $f(u)=\frac{1}{\sqrt{u}}, u>0$, the Taylor series of $f(u)$ at center c is expressed

$$f(u) = \frac{1}{\sqrt{c}}\left[1+\sum_{m=1}^{\infty}\frac{(2\mathrm{m}-1)!!}{(2\mathrm{m})!!}\left(1-\frac{u}{c}\right)^m\right], \tag{A-7}$$

where $(2\mathrm{m}-1)!! = 1\cdot 3\cdot 5\ldots(2\mathrm{m}-1)$, $(2\mathrm{m})!! = 1\cdot 3\cdot 5\ldots(2\mathrm{m})$. Consequently, the signum function $\mathrm{sgn}x$ is expressed

$$\mathrm{sgn}\,x = \frac{x}{\sqrt{c}}\left[1+\sum_{m=1}^{\infty}\frac{(2\mathrm{m}-1)!!}{(2\mathrm{m})!!}\left(1-\frac{x^2}{c}\right)^m\right]. \tag{A-8}$$

We substitute sinω for x, based on sgnω=sgn(sinω) for $\pi < \omega < \pi$, truncate the series at the first M terms, and obtain the sinusoidal power series of the signum function as

$$\mathrm{sgn}\,\omega = \frac{\sin\omega}{\sqrt{c}}\left[1+\sum_{m=1}^{M}\frac{(2m-1)!!}{(2m)!!}\left(1-\frac{\sin^2\omega}{c}\right)^m + \circ((1-\frac{\sin^2\omega}{c})^{M+1})\right] \quad \text{(A-9)}$$

The series in A-9 converges for $-1 < 1 - \dfrac{\sin\omega}{c} < 1$; that is, c has to be larger than 1/2. On the other hand, the expansion center c in the x-domain is associated to the frequency center in the ω-domain via the relation $c = \sin^2\omega_c$. Therefore, $c = \sin^2\omega_c$ must be less than or equal to 1. Accordingly, c is constrained by $1/2 < c \leq 1$ and the corresponding ω_c is within the range $[\pi/4, \pi/2]$. Clearly, the ideal frequency response is well approximated within the middle frequency band. Multiplying A-9 by $-i$ and substituting $\dfrac{z-z^{-1}}{2i}$ for sinω, the transfer function for the zero phase FIR of the Hilbert transform is expressed as

$$H_{HT}(z,c) \approx -\frac{z-z^{-1}}{2\sqrt{c}}\left\{1+\sum_{m=1}^{M}\frac{(2m-1)!!}{(2m)!!}\left[1+\frac{1}{c}\left(\frac{z-z^{-1}}{2}\right)^2\right]^m\right\} \quad \text{(A-10)}$$

To obtain the causal transfer function, $H_{HT}(z,c)$ is multiplied by z^{-2M-1} and the resultant transfer function of the FIR Hilbert transform of the $(2M+2)$th-order is

$$\hat{H}_{HT}(z,c) \approx -\frac{1-z^{-2}}{2\sqrt{c}}\left\{z^{-2M}+\sum_{m=1}^{M}\frac{(2m-1)!!}{(2m)!!}z^{-2(M-m)}\left[z^{-2}+\frac{1}{c}\left(\frac{1-z^{-2}}{2}\right)^2\right]^m\right\} \quad \text{(A-11)}$$

For M=0, the transfer functions of equations A-4 and A-11 are approximated as

$$\hat{H}_{HT}(z,c) \approx -\frac{1-z^{-2}}{2\sqrt{c}} \quad \text{(A-12)}$$

$$\hat{F}_{DD}(z) \approx -\frac{1-z^{-2}}{2} \quad \text{(A-13)}$$

We compare equations A-12 and A-13, and we conclude that these two transfer functions in middle frequency band of the frequency domain differ by the constant coefficient $\dfrac{1}{\sqrt{c}}$.

REFERENCES

Bekara, M., and M. van der Baan, 2009, Random and coherent noise attenuation by empirical mode decomposition: Geophysics, **74**, V89–V98.

Fehmers, G. C., and C. F. W. Hocker, 2003, Fast structural interpretation with structure-oriented filtering: Geophysics, **68**, 1286–1293.

Fomel, S., 2002, Applications of plane-wave destruction filters: Geophysics, **67**, 1946–1960.

———, 2007, Shaping regularization in geophysicalestimation problems: Geophysics, **72**, R29–R36.

———, 2009, Adaptive multiple subtraction using regularized nonstationary regression: Geophysics, **74**, V25–V33.

Fomel, S., and A. Guitton, 2006, Regularizing seismic inverse problems by model reparameterization using plane-wave construction: Geophysics, **71**, A43–A47.

Hoeber, H. C., S. Brandwood, and D. N. Whitcombe, 2006, Structurally consistent filtering: In 68th EAGE Conference Exhibition.

Lehmer, D. C., 1985, Interesting series involving the central binomial coefficient: American Mathematical Monthly.

Li, H. S., G. C. Wu, and X. Y. Yin, 2012, Application of morphological component analysis to remove of random noise in seismic data: Journal of Jilin University(Earth Science Edition), **42**, 554–561.

Li, Y., B. J. Yang, and H. B. L. et al., 2013, Suppression of strong random noise in seismic data by using timefrequency peak filtering: Science China Earth Sciences, **56**, 1200–1208.

Liu, C., Y. Liu, B. J. Yang, D. Wang, and J. G. Sun, 2006, A 2D multistage median filter to reduce random seismic noise: Geophysics, **71**, 105–110.

Liu, G., and X. Chen, 2013, Noncausal f-x-y regularized nonstationary prediction filtering for random noise attenuation on 3d seismic data: Journal of Applied Geophysics, **93**, 60–66.

Liu, G. C., X. H. Chen, J. Y. Li, and et al., 2011a, Seismic noise attenuation using nonstationary polynomial fitting: Applied Geophysics, **8**, 18(C26.

Liu, Y., S. Fomel, C. Liu, and et al., 2009a, High-order seislet transform and its application of random noise attenuation: Chinese Journal of Geophysics, **52**, 2142–2151.

Liu, Y., S. Fomel, and G. Liu, 2010, Nonlinear structureenhancing filtering using plane-wave prediction: Geophysical Prospecting, **58**, 415–427.

Liu, Y., C. Liu, and D. Wang, 2009b, A 1D time-varying median filter for seismic random, spike-like noise elimination: Geophysics, **74**, 17–24.

Liu, Y., D. Wang, and C. Liu, 2011b, Weighted median filter based on local correlation and its application to poststack random noise attenuation: Chinese Journal of Geophysics, **54**, 358–367.

Liu, Z., W. Zhao, and X. Chen, 2012, Local svd for random noise suppression of seismic data in frequency domain: Oil Geophysical Prospecting, **47**, 202–206.

Lu, Y. H., and W. K. Lu, 2009, Edge-preserving polynomial fitting method to suppress random seismic noise: Geophysics, **74**, V69–V73.

Maraschini, M., and C. G. G. N. Turton, 2013, Assessing the impact of a non-local-means random noise attenuator on coherency: SEG Technical Program Expanded Abstracts.

Ottolini, R., 1983, Signal/noise separation in dip space: SEP Report, **37**.

Pei, S. C., and P. H. Wang, 2001, Closed-form design of maximally flat fir hilbert transformers, differentiators, and fractional delayers by power series expansion:

IEEE Transactions on, Circuits and Systems I: Fundamental Theory and Applications, **48**, 389–398.

Schleicher, J., J. C. Costa, and L. T. Santos, 2009, On the estimation of local slopes: Geophysics, **74**, P25–P33.

Tikhonov, A., 1963, Solution of incorrectly formulated problems and the regularization method: In Soviet Math.Dokl.